



ELSEVIER

Available online at [www.sciencedirect.com](http://www.sciencedirect.com)

SCIENCE @ DIRECT®

**NUCLEAR  
INSTRUMENTS  
& METHODS  
IN PHYSICS  
RESEARCH**  
Section A

Nuclear Instruments and Methods in Physics Research A 551 (2005) 528–539

[www.elsevier.com/locate/nima](http://www.elsevier.com/locate/nima)

# Heavy-ion-induced production and physical preseparation of short-lived isotopes for chemistry experiments

Ch.E. Düllmann<sup>a,b,\*</sup>, C.M. Folden III<sup>a,b</sup>, K.E. Gregorich<sup>a</sup>, D.C. Hoffman<sup>a,b</sup>,  
D. Leitner<sup>a</sup>, G.K. Pang<sup>a,b</sup>, R. Sudowe<sup>a</sup>, P.M. Zielinski<sup>a,b</sup>, H. Nitsche<sup>a,b</sup>

<sup>a</sup>*Nuclear Science Division, Lawrence Berkeley National Laboratory, Berkeley, CA 94720, USA*

<sup>b</sup>*Department of Chemistry, University of California, Berkeley, CA 94720-1460, USA*

Received 4 March 2005; received in revised form 17 May 2005; accepted 18 May 2005

Available online 18 July 2005

## Abstract

Physical separation of short-lived isotopes produced in heavy-ion-induced fusion reactions is a powerful and well-known method and often applied in investigations of the heaviest elements, called the transactinides ( $Z \geq 104$ ). By extracting these isotopes from a recoil separator, they can be made available for transport to setups located outside the heavily shielded irradiation position such as chemistry setups. This physical preseparation technique overcomes many limitations currently faced in the chemical investigation of transactinides. Here we describe the basic principle using relatively short-lived isotopes of the lighter group 4 elements zirconium (Zr) and hafnium (Hf) used as analogs of the lightest transactinide element, rutherfordium (Rf, element 104). The Zr and Hf isotopes were produced at the LBNL 88-Inch Cyclotron using a cocktail of  $^{18}\text{O}$  and  $^{50}\text{Ti}$  beams and the appropriate targets. Subsequently, the isotopes were physically separated in the Berkeley Gas-filled Separator (BGS) and guided to a Recoil Transfer Chamber (RTC) to transfer them to chemistry setups. The magnetic rigidities of the reaction products in low-pressure helium gas were measured and their identities determined with  $\gamma$ -spectroscopy.

Using preseparated isotopes has the advantages of low background and beam plasma free environment for chemistry experiments. The new possibilities that open up for chemical investigations of transactinide elements are described.

The method can readily be applied to homologous elements within other groups in the periodic table.

© 2005 Elsevier B.V. All rights reserved.

*PACS:* 25.70.Gh; 25.70.Jj; 29.25.Rm

*Keywords:* Cocktail beam; Physical preseparation; Recoil separator; Recoil transfer chamber; Chemistry of transactinides

\*Corresponding author. Lawrence Berkeley National Laboratory, One Cyclotron Road MS 88R0192, Berkeley, CA 94720, USA.  
Tel.: +1 510 486 5052; fax: +1 510 486 7983.

E-mail address: [CEDuellmann@lbl.gov](mailto:CEDuellmann@lbl.gov) (Ch.E. Düllmann).

## 1. Introduction

The experimental investigation of the chemical behavior of the transactinide (TAN) elements ( $Z \geq 104$ ) is an active and interesting field of current research. Chemistry experiments have been concentrated on the lighter TANs and their properties in selected systems in the gas and aqueous phase have been measured. A recent review can be found in Ref. [1]. TAN isotopes are produced as evaporation residues (EVRs) in heavy-ion-induced fusion reactions. In order to overcome many of the limitations currently faced in TAN chemistry research, we introduce the concept of physical preseparation where the EVRs are separated from the beam and unwanted reaction products in a physical recoil separator. They are extracted from the separator and made available for transport to a chemistry setup, usually by means of a gas-jet [2–4]. The beam-free environment in the gas volume at the exit of the separator as well as the suppression of unwanted by-products of the nuclear reaction allow for the investigation of the TAN elements in new, previously inaccessible chemical systems. We will discuss some current experimental methods in the chemical investigation of TAN and the limitations that prevent more detailed studies in Section 2. Then, we will describe how the technique of physically preseparating the isotopes overcomes many of these limitations and highlight a few situations where the method is most useful in the chemical investigation of TANs and short-lived isotopes in general. Section 3 details this concept in one example, namely the production of preseparated isotopes of zirconium (Zr) and hafnium (Hf), the lighter homologs of rutherfordium (Rf), at the Lawrence Berkeley National Laboratory using the 88-Inch Cyclotron and the Berkeley Gas-filled Separator (BGS). Sections 4–6 highlight specific aspects of the new technique and Section 7 contains the conclusions.

## 2. Physical preseparation for chemistry experiments

All TAN isotopes to date have been produced in heavy-ion-induced fusion reactions. In many TAN chemistry experiments, the nuclear reaction pro-

ducts recoiling out of a thin target were stopped directly behind the target and attached to the surface of aerosol particles suspended in a gas volume held at a pressure of about 1–2 bar. These particles were then transported through a capillary in rapidly flowing gas to a chemistry setup located outside the shielding placed around the irradiation position. This technique is referred to as an aerosol-gas-jet [2–4]. In gas-phase experiments, carbon aerosol particles suspended in a carrier gas were usually employed [5]. In the chemistry setup, the particles were converted to gaseous species and thus released the transported radionuclides. In solution chemistry experiments such as solvent extraction [6,7] or ion exchange chromatography studies [8], aerosol particles of soluble materials like KCl were used.

In some gas-phase studies, volatile compounds were formed directly behind the target by thermalizing the recoiling products of the nuclear reaction in a gas that is enriched in a reactive component, such as chlorinating agents [9] or oxygen [10–12]. The gaseous molecules were transported with a carrier gas without being attached to aerosol particles. Both of these techniques, transport with an aerosol-gas-jet and in the form of a volatile compound, permitted the investigation of simple inorganic compounds such as halides or oxides. More complex organometallic molecules and others that are thermally unstable could so far not be investigated by either of these approaches. In experiments using an aerosol-gas-jet, a high-temperature oven ( $T > 800^\circ\text{C}$ ) is used to destroy the aerosol particles in order to release the transported radionuclides. The high temperature prevents the formation and study of the thermally unstable compounds. When a pure-gas-jet system without aerosol particles is used, volatile species are produced in the recoil chamber directly behind the target and then transported out of the chamber. In this case, thermally unstable compounds would be immediately destroyed by the plasma behind the target caused by the intense heavy-ion beam [13]. Adding such compounds outside the recoil chamber as was done in Ref. [13] is expected to result in reduced yields. As a consequence of all these limitations, only few chemical systems such as the group 4 chlorides

[14], group 6 oxychlorides [9] or group 8 oxides [10,12] could be studied with this approach.

One major problem in many TAN chemistry experiments is the substantial amount of nuclear transfer products produced in incomplete fusion reactions as well as products of the interaction of the beam with the target assembly and impurities in the target. The resulting background arises from isotopes of elements from many different groups of the periodic table. Some of these isotopes may exhibit decay properties similar to the TAN element of interest and complicate or even render impossible its unambiguous identification. In past experiments, choice of a chemical system was dominated by the need for a good separation from these elements, which necessitated favoring selectivity between different groups of the periodic table over selectivity between the different members of a given group. The differences in chemical behavior among the different elements in the same group could thus only be studied in limited detail.

In the preceding paragraphs, we have identified four major limitations of the currently employed techniques for chemically investigating TANs: (i) the plasma behind the target caused by the intense heavy-ion beam, (ii) the high temperature needed to release radionuclides adsorbed on aerosol particles in gas-phase studies with an aerosol-gas-jet, (iii) high background rates from interfering byproducts of the nuclear production reaction, and (iv) the need for chemical systems that favor separation of elements of the investigated group of the periodic table from all other elements over selectivity between group members, thus limiting the available chemical systems dramatically.

All of these limitations can be overcome by employing physical preseparation of the desired nuclear reaction products formed as evaporation residues (EVRs) in heavy-ion-induced fusion reactions. In this technique, a physical device such as a gas-filled magnetic separator or a vacuum separator comprising electrostatic and/or magnetic deflection elements is used to remove the intense heavy-ion beam and a substantial fraction of the nuclear transfer products from the desired radionuclide. The separation is based on differences in magnetic rigidity, electric rigidity, or velocity. The desired atoms are guided to a so-called Recoil

Transfer Chamber (RTC) [15] which transfers the separated EVRs to the appropriate chemistry setup. The RTC consists of a gas-filled (usually 1–2 bar) chamber mounted at the focal plane of the separator and is isolated from its vacuum chamber or low-pressure (0.5–1 mbar) filling gas by a thin Mylar foil referred to as the RTC window. The transport from the RTC to the chemistry apparatus can be performed, e.g., by using a gas-jet (either with or without aerosol particles). In contrast to experiments without preseparation where thermally unstable compounds were added to the carrier gas outside the recoil chamber, these can now be fed directly into the RTC which is expected to lead to increased yields. Removal of most unwanted elements, which was not possible in Ref. [13], is performed in the separator. In contrast to conventional chemistry experiments without preseparation, where targets with thicknesses up to  $1.5 \text{ mg/cm}^2$  have been used, only rather thin targets with thicknesses up to about  $500 \text{ }\mu\text{g/cm}^2$  can be used for preseparation due to the acceptance limitations of the physical separators. Together with losses due to separator efficiency, this can lead to production rates that are smaller than in experiments without preseparation. However, this possible limitation is usually outweighed by the advantages of our method.

So far, only one TAN element has been chemically investigated using preseparated isotopes [16,17] and the Berkeley Gas-filled Separator (BGS) [18] installed at the Lawrence Berkeley National Laboratory (LBNL) was used as a physical separator. In these liquid–liquid extraction experiments, the behavior of Rf was studied and compared to its lighter homologs Hf and Zr, which were investigated in separate studies. Use of preseparated isotopes resulted in nearly background-free experiments which enabled unambiguous identification of  $^{257}\text{Rf}$  ( $T_{1/2} = 4.3 \text{ s}$ ), which had previously not been possible [19].

Chemical investigations of the TAN elements usually compare their behavior to that of their lighter homologs in the periodic table. The most accurate comparisons can be obtained when all studied elements are produced and investigated simultaneously. The influence of

differing experimental conditions, which can lead to irreproducible results and erroneous conclusions, is an important factor to consider when assessing the results of studies where the compared elements have not been investigated simultaneously. The transport yield of aerosol-gas-jets, for example, is often not reproducible, which is disadvantageous for studies that depend on a constant production and transport yield. Other examples of differences in gas-phase experiments are unequal surface conditions or different trace amounts of reactive impurities (e.g., oxygen or water) which are less important in studies of macroamounts. In liquid-phase experiments, differences in the size and composition of the aerosol particles may affect their solubility. It is also preferable to use the same solutions for all chemistry experiments since aging effects (e.g., uptake of oxygen or carbondioxide) can alter the results. All such problems can be avoided by direct comparison of all the elements under study in the same experiment. This is commonly done by irradiating targets containing a mixture of different elements that lead to the production of all homologs using the same projectile.

However, when physical preseparation, which is based on differences in magnetic (as in case of the BGS) or electric rigidity or in velocity, is employed, these isotopes cannot be guided to the RTC simultaneously. Additionally, the BGS is not suited for separating Zr isotopes produced in almost symmetric (e.g., Ti-induced) nuclear reactions. This is due to the very similar magnetic rigidities of the beam and evaporation residues in this reaction type which make a separation of the two impossible. Choosing more asymmetric reactions, e.g., based on  $^{18}\text{O}$  as a common projectile, is generally undesirable, since the slow Hf and Rf EVRs produced in such reactions cannot penetrate the Mylar foil used as the RTC window. The minimum thickness of this foil is defined by the maximum acceptable leakage from the high-pressure chemistry side into the separator and is an even bigger concern should a vacuum separator be used instead of a gas filled one. In case of the BGS and the current RTC window design, a limit of about  $2.5\mu\text{m}$  was determined for Mylar. It follows that it is not possible to investigate Zr, Hf,

and Rf simultaneously when isotopes pre-separated in the BGS are used.

The next best approach is switching between short-lived isotopes of these elements without long delay times and without having to open or change any part of the experimental setup, minimizing variations in experimental conditions in studies of the different homologous elements. This can be achieved when isotopes of all these elements are produced in heavy-ion-induced fusion reactions employing projectiles of similar  $E/m$  and  $m/q$ , where  $E$  is the beam energy in the lab frame,  $m$  the mass, and  $q$  the charge state. Such projectiles can be simultaneously injected into a cyclotron and switching from one beam to the other can be achieved solely by adjusting the frequency of the cyclotron, which is fast if the  $m/q$  difference is small. This near-simultaneous acceleration of different ions is referred to as a “heavy-ion cocktail” and similar cocktails are already routinely employed at the LBNL 88-Inch Cyclotron for applied research [20]. The kinematic differences of the nuclear reactions lead to different recoil ranges of isotopes of different elements. In order to compensate for this effect, fast EVRs are degraded so their recoil range matches the one of the slowest EVRs. In the work presented here the technique was used for the near-simultaneous production and preseparation of short-lived Zr and Hf isotopes. This allows the study of the chemistry of these elements on an atom-at-a-time level and development of a chemical system that can be used in a future experiment where the three group 4 homologs, Zr, Hf, and Rf, are investigated in one single experiment. Switching from the production of Zr to Hf involves (i) changing the beam, (ii) changing the target (since no mixed targets were used), (iii) changing the BGS magnet settings, and (iv) introducing or removing a Mylar degrader foil. The time required for these changes is usually about 15 min. A slight increase in beam energy over the value used here, which does not affect the conclusions of this work, allows for the production of all three elements including Rf. The method can be applied to homologous elements within other groups of the periodic table without major conceptual changes.

### 3. Near-simultaneous production of physically pre-separated isotopes

#### 3.1. The cocktail beam

A cocktail beam of  $^{18}\text{O}^{4+}$  and  $^{50}\text{Ti}^{11+}$  was developed using isotopically enriched metallic  $^{50}\text{Ti}$  and gaseous  $^{18}\text{O}_2$ . The particles were extracted from the LBNL ECR ion source [21], injected into the 88-Inch Cyclotron and accelerated to about 4.6 MeV/u. By varying the cyclotron frequency, either the 83.6-MeV  $^{18}\text{O}^{4+}$  or the 228.0-MeV  $^{50}\text{Ti}^{11+}$  projectiles were extracted. The pertinent parameters of the beams are summarized in Table 1. As the difference in the cyclotron frequency of the two beams is larger than the  $\sim 5$  kHz resonance width of the 88-Inch Cyclotron, they are isotopically pure.

#### 3.2. The Berkeley Gas-filled Separator (BGS) as a physical preseparator

A schematic of the experimental setup is displayed in Fig. 1. Short-lived isotopes of Zr and Hf were produced in heavy-ion-induced reactions of  $^{18}\text{O}$  with a  $^{\text{nat}}\text{Ge}$  or an enriched  $^{74}\text{Se}$  target, and reactions of  $^{50}\text{Ti}$  with targets of enriched Sn isotopes, respectively. The beam passed through a (40–45)- $\mu\text{g}/\text{cm}^2$  carbon vacuum window and a negligible amount of helium (He) before entering the target. Isotopically enriched targets of  $^{74}\text{Se}$ ,  $^{112}\text{Sn}$ ,  $^{116}\text{Sn}$ ,  $^{120}\text{Sn}$ ,  $^{124}\text{Sn}$ , as well as  $^{\text{nat}}\text{Ge}$ , all in the elemental form, were used. They were produced by vacuum deposition from a resistance heated source. Up to five targets were mounted on a sliding ladder that allowed for the

desired target to be positioned in the path of the beam without opening the system.

The desired products of the nuclear reactions were separated from the beam and the majority of the nuclear transfer products by the BGS [18]. The BGS was filled with 0.7 mbar He. The magnetic rigidities of the major EVRs were measured in a silicon strip detector positioned in the focal plane of the BGS. Each of the eight individual strips was 10 mm wide  $\times$  35 mm high and was position sensitive in the vertical direction. The whole detector was 80 mm wide  $\times$  35 mm high. It was calibrated using an external  $\alpha$ -source containing  $^{148}\text{Gd}$  ( $E_\alpha = 3183$  keV),  $^{239}\text{Pu}$  ( $E_\alpha = 5157$  keV),  $^{241}\text{Am}$  ( $E_\alpha = 5486$  keV), and  $^{244}\text{Cm}$  ( $E_\alpha = 5805$  keV). The magnetic rigidities were extracted from the magnet settings at which the EVR distribution was centered in the focal plane. The velocities (in units of the Bohr velocity  $v_0$ , which is the classical velocity of the 1 s electron in the hydrogen atom) and magnetic rigidities of the main EVRs of all studied beam/target combinations are given in Table 2.

#### 3.3. Zirconium: $^{85}\text{Zr}$

Relative production rates of  $^{85}\text{Zr}$  ( $T_{1/2} = 7.9$  min,  $E_\gamma = 454$  keV,  $I_{454} = 45\%$ ) for the two reactions  $^{\text{nat}}\text{Ge}(^{18}\text{O}, xn)^{85}\text{Zr}$  and  $^{74}\text{Se}(^{18}\text{O}, \alpha 3n)^{85}\text{Zr}$  at a lab frame beam energy of 82.5 MeV were estimated using the codes HIVAP [22,23] and EVAPOR [24] and are given in Table 3. In the first case, the two reactions  $^{70}\text{Ge}(^{18}\text{O}, 3n)$  and  $^{72}\text{Ge}(^{18}\text{O}, 5n)$  are predicted by HIVAP to be the main contributors to the  $^{85}\text{Zr}$  production. Based on these results and the estimated efficiency [25] of the BGS for guiding the produced EVRs to the 150 mm wide  $\times$  80 mm high RTC window, the  $^{74}\text{Se}$ -based reaction was expected to yield four times as much  $^{85}\text{Zr}$  as the  $^{\text{nat}}\text{Ge}$ -based one.

Targets of 350  $\mu\text{g}/\text{cm}^2$   $^{\text{nat}}\text{Ge}$  deposited on 45- $\mu\text{g}/\text{cm}^2$  carbon backings and 384  $\mu\text{g}/\text{cm}^2$   $^{74}\text{Se}$  deposited on 40- $\mu\text{g}/\text{cm}^2$  carbon backings were irradiated. The  $^{74}\text{Se}$  targets were covered with a 50- $\mu\text{g}/\text{cm}^2$  thick gold (Au) layer on the downstream side to prevent loss of target material due to sputtering and evaporation during the irradiations. Typical beam intensities for measurements with the silicon strip detector were (10–100) particle pA

Table 1  
Parameters of the ions used in the cocktail beam

Projectile	$E$ (MeV)	$E/m$ (MeV/u)	$m/q$	Frequency (MHz)
$^{18}\text{O}^{4+}$	83.6	4.645	4.50	14.5162
$^{50}\text{Ti}^{11+}$	228.0	4.565	4.54	14.3875

The second column gives the energy of the beam delivered by the LBNL 88-Inch Cyclotron.  $E$  denotes the energy in the lab frame,  $m$  is the mass of the projectile, and  $q$  the charge state. The cyclotron frequency (3rd harmonic frequency mode) is given in the last column.



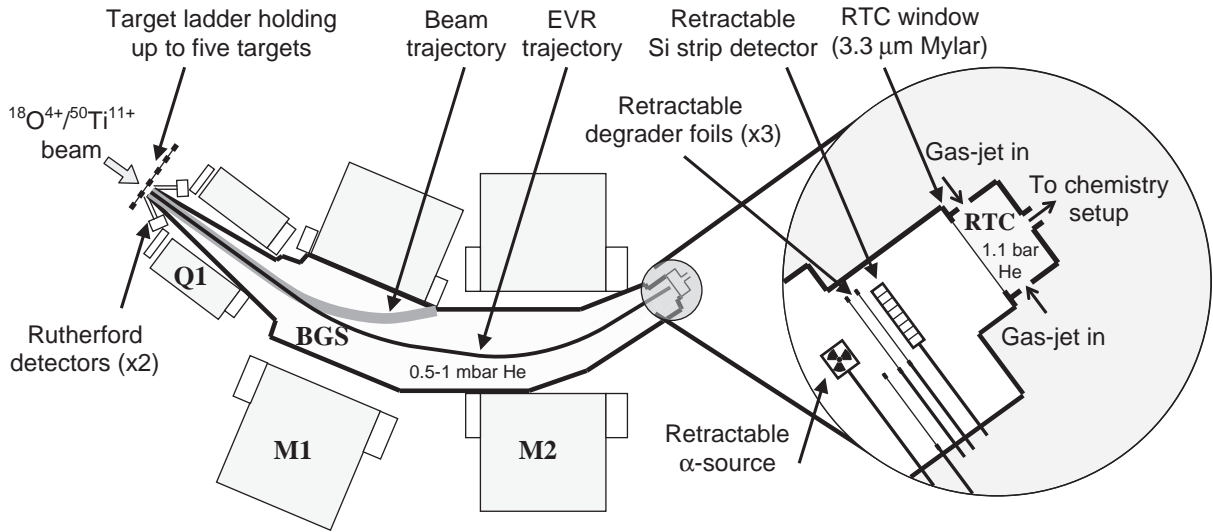


Fig. 1. Schematic of the BGS experimental setup. One of the two beams of the  $^{18}\text{O}^{4+}/^{50}\text{Ti}^{11+}$  cocktail accelerated by the LBNL 88-Inch Cyclotron is delivered to the target position. Up to five targets can be installed on a slider that allows for the desired target to be positioned in the path of the beam without opening the system. The produced EVRs are spatially separated from the beam and nuclear transfer products in the BGS which is filled with 0.7 mbar of He. An enlarged view of the focal plane area at the exit of the BGS is displayed in the circle on the right of the figure. A retractable Si strip detector with eight strips that are position sensitive in the vertical direction allows measurement of magnetic rigidities of EVRs to verify that their distribution is centered in the focal plane. The detector is calibrated with a retractable  $\alpha$ -particle source. Both the detector and the source are moved out of the path of the EVRs to allow them to reach the RTC which is separated from the BGS by the RTC window. The velocity of EVRs entering the RTC can be reduced by introducing up to three degrader foils into the path of the EVRs inside the BGS. Inside the RTC, the EVRs are available for transport to a chemistry apparatus, e.g., by using a gas-jet.

Table 2  
Kinematic parameters and measured magnetic rigidities of the main reaction products

Beam	Target	$E_{\text{Beam}}$ (MeV)	EVR of interest	Velocity ( $v/v_0$ )	$B \cdot \rho$ (T m)
$^{18}\text{O}$	$^{\text{nat}}\text{Ge}$	82.8	$^{85}\text{Zr}$ (7.86 min)	2.72–2.78 <sup>a</sup>	0.92
$^{18}\text{O}$	$^{74}\text{Se}$	82.7	$^{85}\text{Zr}$ (7.86 min)	2.77	0.92
$^{50}\text{Ti}$	$^{112}\text{Sn}$	223.0	$^{158}\text{Hf}$ (2.85 s)	4.13	1.41
$^{50}\text{Ti}$	$^{116}\text{Sn}$	224.4	$^{162}\text{Hf}$ (37.6 s)	4.05	1.44
$^{50}\text{Ti}$	$^{120}\text{Sn}$	224.1	$^{165}\text{Hf}$ (76 s)	3.95	1.50
$^{50}\text{Ti}$	$^{124}\text{Sn}$	223.7	$^{169}\text{Hf}$ (3.24 min)	3.86	1.56

The third column gives the energy of the beam in the center of the target in the lab frame. Energy losses inside the vacuum window, target backing, and target material were calculated with SRIM-2003 [27]. Different energies for the same beam are mainly caused by different target thicknesses. The fifth column lists the velocities of the EVRs of interest in units of the Bohr velocity  $v_0$  ( $v_0 \approx 2.2 \times 10^6$  m/s). The measured magnetic rigidity is listed in the last column.

<sup>a</sup>The reactions  $^{70}\text{Ge}(^{18}\text{O},3n)$  and  $^{72}\text{Ge}(^{18}\text{O},5n)$  were considered.

$(6.2 \times 10^7 - 6.2 \times 10^8$  particles/s). The spectra in the focal plane showed the impact of EVRs with a recorded pulse height of around 10 MeV and a substantial amount of scattered beam with a recorded

pulse height of about 90 MeV, indicating that the BGS is not very well suited for separating products of such light nuclear reactions as  $\text{O} + \text{Ge}/\text{Se}$ . The deduced beam separation factor was of the

Table 3

Predictions of production cross-sections using the codes HIVAP [22,23] and EVAPOR [24] for the reactions  $^{nat}\text{Ge}(^{18}\text{O},xn)$  and  $^{74}\text{Se}(^{18}\text{O},\alpha 3n)$

Target	Reaction	$\sigma$ (HIVAP) (mbarn)	$\sigma$ (EVAPOR) (mbarn)	BGS efficiency	Expected rel. yield	Measured rel. yield
$^{70}\text{Ge}$	3n	44.3	31.0			
$^{72}\text{Ge}$	5n	34.8	15.9			
$^{73}\text{Ge}$	6n	2.6	2.4			
$^{nat}\text{Ge}$	xn	19.2	11.15	~40%	23	100
$^{74}\text{Se}$	$\alpha 3n$		193.4	~10%	100	25–50

The BGS efficiency was estimated with the method described in Ref. [25]. The last two columns list the expected and measured relative yield of  $^{85}\text{Zr}$  at the exit of the BGS for the two reactions. In the calculations with the  $^{nat}\text{Ge}$  target,  $^{85}\text{Zr}$  formed in reactions with the isotopes  $^{70}\text{Ge}$ ,  $^{72}\text{Ge}$ , and  $^{73}\text{Ge}$  was considered.

order of  $10^5$ ; the ratio of registered beam particles to EVRs was about 6–8. The EVR distribution was very wide, much wider than the width of the focal plane detector. Since all the nuclear reaction products of the reactions of  $^{18}\text{O}$  with  $^{nat}\text{Ge}$  and  $^{74}\text{Se}$  decay by  $\beta^+$ -decay and electron-capture (EC) (to which the focal plane detector is not sensitive) only their entry into the detector could be registered. Their identity was determined in measurements of their  $\gamma$ -rays. These experiments are described in Section 5.

### 3.4. Hafnium: $^{158,162,165,169}\text{Hf}$

The option to investigate several isotopes exhibiting different decay properties is very useful in the preparation of experiments with TAN isotopes. The combination of a  $^{50}\text{Ti}$  beam and any of the stable Sn isotopes with masses between 112 and 124 permits production of different Hf isotopes with half-lives that cover a wide range, without changing the beam energy.  $^{169}\text{Hf}$  ( $T_{1/2} = 3.2$  min,  $E_\gamma = 493$  keV,  $I_{493} = 84\%$ ),  $^{165}\text{Hf}$  ( $T_{1/2} = 76$  s,  $E_\gamma = 180$  keV,  $I_{180\text{rel}} = 100\%$ ), and  $^{162}\text{Hf}$  ( $T_{1/2} = 38$  s,  $E_\gamma = 174$  keV,  $I_{174\text{rel}} = 100\%$ ) are well suited for measurement with a  $\gamma$ -detector. These nuclides are appropriate for developing a chemical system for use with  $^{261\text{m}}\text{Rf}$  ( $T_{1/2} = 78$  s) due to their similar half-lives. On the other hand, the  $\alpha$ -branch of 44% ( $E_\alpha = 5.268$  MeV) and relatively short half-life of  $^{158}\text{Hf}$  ( $T_{1/2} = 2.6$  s) make this a good model isotope for optimization of a system for the short-lived  $^{257}\text{Rf}$  ( $T_{1/2} = 4.3$  s).

The following targets were irradiated in these studies:  $470\text{ }\mu\text{g}/\text{cm}^2$   $^{112}\text{Sn}$  deposited on a  $\sim 45\text{-}\mu\text{g}/\text{cm}^2$  carbon backing;  $250\text{ }\mu\text{g}/\text{cm}^2$   $^{116}\text{Sn}$  deposited on a  $45\text{-}\mu\text{g}/\text{cm}^2$  carbon backing;  $300\text{ }\mu\text{g}/\text{cm}^2$   $^{120}\text{Sn}$  deposited on a  $45\text{-}\mu\text{g}/\text{cm}^2$  carbon backing; and a self-supporting  $586\text{ }\mu\text{g}/\text{cm}^2$   $^{124}\text{Sn}$  target. Typical beam intensities for measurements with the silicon strip detector were (0.5–2) particle nA ( $3.1 \times 10^9$ – $1.3 \times 10^{10}$  particles/s). All nuclear reaction products of the reactions of  $^{50}\text{Ti}$  with  $^{116,120,124}\text{Sn}$  decay by  $\beta^+$ -emission and EC and only their deposition in the detector could be registered. The identity of the products of the  $^{116,124}\text{Sn}$ -based reactions was determined in experiments where their  $\gamma$ -rays were measured as described in Section 5. In contrast, the reaction with a  $^{112}\text{Sn}$  target produced isotopes with non-negligible  $\alpha$ -branches. An  $\alpha$ - $\alpha$ -correlation analysis of the results revealed decay chains starting with the isotopes  $^{157,158,159}\text{Hf}$  (the products of the 5n, 4n, and 3n exit channels),  $^{157}\text{Lu}$  (p4n), and  $^{156}\text{Yb}$  ( $\alpha 2n$ ). From the ratio of observed  $^{157}\text{Lu}$  and  $^{157}\text{Hf}$  events it follows that most of the  $^{157}\text{Lu}$  is produced directly in the p4n channel. In line with earlier experiments, no full-energy  $^{50}\text{Ti}$  projectiles were detected in the focal plane detector, indicating a beam separation factor in excess of  $10^{11}$ .

### 3.5. Rutherfordium: $^{257}\text{Rf}$

The cocktail technique has so far not been used to produce Zr, Hf, and Rf isotopes in the same experiment and here we introduced the method using Zr and Hf isotopes only. In a future

experiment where all three elements are studied near-simultaneously, the energy of the cocktail will have to be increased slightly to about 4.68 MeV/u for  $^{50}\text{Ti}^{11+}$ , corresponding to  $E_{\text{Lab}} = 233.7$  MeV in order to match the maximum of the excitation function of the  $^{208}\text{Pb}(^{50}\text{Ti},n)^{257}\text{Rf}$  reaction which was measured to be  $(10 \pm 1)$  nb at  $E_{\text{beam}} = 229.7$  MeV (lab frame) in the center of (450–500)- $\mu\text{g}/\text{cm}^2$  thick targets [26]. The same parameters for the vacuum window and target composition as used in Ref. [17] were assumed in this calculation and the energy loss of  $^{50}\text{Ti}$  in the various layers of matter was calculated with SRIM-2003 [27]. The corresponding energy for the  $^{18}\text{O}^{4+}$  beam would be 85.8 MeV.

A rotating  $^{208}\text{Pb}$ -target wheel which can tolerate highly intense beams can be installed between the vacuum window and the target ladder to allow the production of  $^{257}\text{Rf}$  in the reaction  $^{208}\text{Pb}(^{50}\text{Ti},n)^{257}\text{Rf}$ . The ladder is retracted for the Rf studies and inserted again for the studies of Zr and Hf. The beam energy will be slightly lower for the homolog studies due to the energy loss of the beam in the  $^{208}\text{Pb}$  target. According to HIVAP [22,23] calculations, these slight changes of the beam energy should not affect the production rate of Zr and Hf isotopes dramatically, and the near-simultaneous investigation of all three elements is possible with such a cocktail.

#### 4. Design of the RTC window

The interface between the BGS and the gas-filled volume of the RTC [15], which forwards the separated EVRs to a chemistry setup, consists of a thin Mylar foil through which the EVRs penetrate into the RTC. Therefore, the energy loss of the separated recoils of the  $^{50}\text{Ti} + ^{124}\text{Sn}$  and the  $^{18}\text{O} + ^{\text{nat}}\text{Ge}$  reactions in Mylar was measured. Mylar foils of various nominal thicknesses were purchased. Their thicknesses and homogeneities were verified with  $\alpha$ -particle energy loss measurements using an  $\alpha$ -source containing  $^{239}\text{Pu}$ ,  $^{241}\text{Am}$ , and  $^{244}\text{Cm}$ . Foils of the following thicknesses (nominal/measured) were used: 0.9/0.9  $\mu\text{m}$ , 2.0/(not measured)  $\mu\text{m}$ , 2.5/2.4  $\mu\text{m}$ , 3.6/3.3  $\mu\text{m}$ , and 6.0/5.8  $\mu\text{m}$ . The variations of thicknesses of

individual foils were below  $\pm 0.1 \mu\text{m}$ . Various combinations of foils were inserted in the path of the EVRs in front of the focal-plane detector and the residual energies of the EVRs were measured. These values were corrected for pulse-height defect according to Moulton et al. [28] and the results were compared to theoretical estimates obtained for  $^{169}\text{Hf}$  and  $^{85}\text{Zr}$  using SRIM-2003 [27]. The results are displayed in Fig. 2. The range for 55.1-MeV  $^{169}\text{Hf}$  in Mylar is about 13.1  $\mu\text{m}$  based on an extrapolation of the experimental data (dashed line in Fig. 2), in good agreement with the SRIM-2003 calculations which predict a range of 12.4  $\mu\text{m}$ . The range of 13.0-MeV  $^{85}\text{Zr}$  is between 4.2 and 4.7  $\mu\text{m}$  while SRIM-2003 predicts 6.4  $\mu\text{m}$ . Therefore, a 3.3- $\mu\text{m}$  thick Mylar foil was chosen for the RTC window (dotted line in Fig. 2). This foil allows all produced Hf and Zr isotopes to leave the BGS and enter the RTC. A 3.2-mm-thick stainless-steel plate with round holes of 6.25-mm diameter arranged in a hexagonal pattern serves as supporting structure, which enables the window to withstand the pressure difference between the RTC

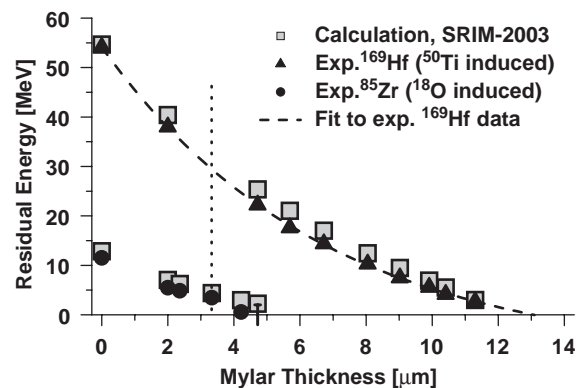


Fig. 2. Residual energies of EVRs produced in the reactions  $^{50}\text{Ti} + ^{124}\text{Sn}$  (▲) and  $^{18}\text{O} + ^{\text{nat}}\text{Ge}$  (●) after passing through Mylar foils of various thicknesses. Some points were obtained by combining two or more foils of appropriate thicknesses. The thicknesses of the foils were verified by measuring the energy loss of  $\alpha$ -particles passing through them. Measured values were corrected for pulse-height defects according to Ref. [28]. Gray squares denote energy loss calculations using the code SRIM-2003 [27]. The dotted line indicates the thickness of the RTC window of 3.3  $\mu\text{m}$ , the extrapolated range of the  $^{50}\text{Ti} + ^{124}\text{Sn}$  residues is indicated by the dashed line.



(1.1 bar) and the BGS (0.7 mbar). The geometric transparency of the grid is 79.7%.

### 5. $\gamma$ -spectroscopic determination of the produced isotopes

The focal-plane detector was retracted and moved out of the path of the EVRs, allowing them to pass through the Mylar foil and into the RTC, where they were thermalized in 1.1 bar He. The EVRs produced in  $^{50}\text{Ti}$ -induced reactions have a relatively long range. Therefore, they were degraded by passing through 5.7- $\mu\text{m}$  thick Mylar foils installed in front of the RTC window (3.3- $\mu\text{m}$  Mylar) allowing them to thermalize in the 1.1 bar He in the 40-mm-deep RTC. The EVRs were then available for transport to a chemistry system. To determine which isotopes stopped in the RTC, they were attached to KCl aerosol particles and transported with a rapid gas flow through a stainless-steel capillary (length:  $\sim 20$  m, i.d.  $\sim 2$  mm) to a filter consisting of glass fiber and activated charcoal, where they were trapped. That filter was placed in front of a HPGe  $\gamma$ -detector. The aerosol was produced by feeding 1.5–1.7 l/min He through an oven (640  $^{\circ}\text{C}$ ) containing a KCl-laden crucible. The transport efficiency of such KCl/He aerosol-gas-jets has been measured in separate experiments to be about 70%. The spectra obtained in the reactions  $^{18}\text{O} + ^{\text{nat}}\text{Ge}$ ,  $^{18}\text{O} + ^{74}\text{Se}$ ,  $^{50}\text{Ti} + ^{124}\text{Sn}$ , and  $^{50}\text{Ti} + ^{116}\text{Sn}$  are displayed in Figs. 3 and 4. The beam intensities were 75 particle nA ( $4.7 \times 10^{11}$  particles/s) for the  $^{18}\text{O}$ -induced reactions and 30 particle nA ( $1.9 \times 10^{11}$  particles/s) for the  $^{50}\text{Ti}$ -induced reactions, respectively. No notable loss of target material was observed in these experiments where relatively high beam intensities were used.

The  $\gamma$ -spectra of the two reactions used for producing  $^{85}\text{Zr}$  (Fig. 3) show that both of these reactions are suitable. However, the amount of  $^{85}\text{Zr}$  entering the RTC is about a factor of two to four smaller for the  $^{74}\text{Se}$ -based reaction than for the  $^{\text{nat}}\text{Ge}$ -based reaction after correcting for differing beam intensities and target thicknesses. This is in contrast to the increase of about a factor of four, which was expected from calculations for

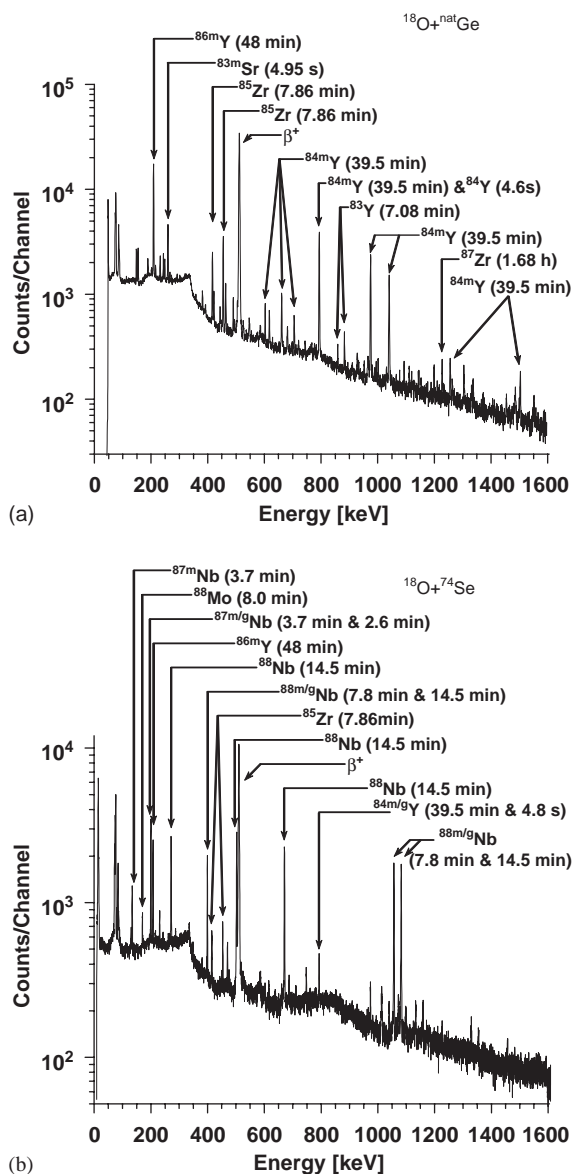


Fig. 3.  $\gamma$ -ray spectra obtained in the reactions (a)  $^{18}\text{O} + ^{\text{nat}}\text{Ge}$  and (b)  $^{18}\text{O} + ^{74}\text{Se}$  used for the production of  $^{85}\text{Zr}$  ( $T_{1/2} = 7.9$  min). All nuclear reaction products were attached to KCl aerosol particles and transported with a KCl/He aerosol-gas-jet to a glass-fiber/activated charcoal filter which was monitored with a HPGe  $\gamma$ -detector. Acquisition of the spectra was started 6 min after the start of bombardment. Measuring time was 30 min, while the beam was on. The relevant  $\gamma$ -lines are labeled.

the  $^{74}\text{Se}$ -based reaction (see Table 3). Whether the discrepancy is mainly due to differences between estimated and real (i) production cross-sections

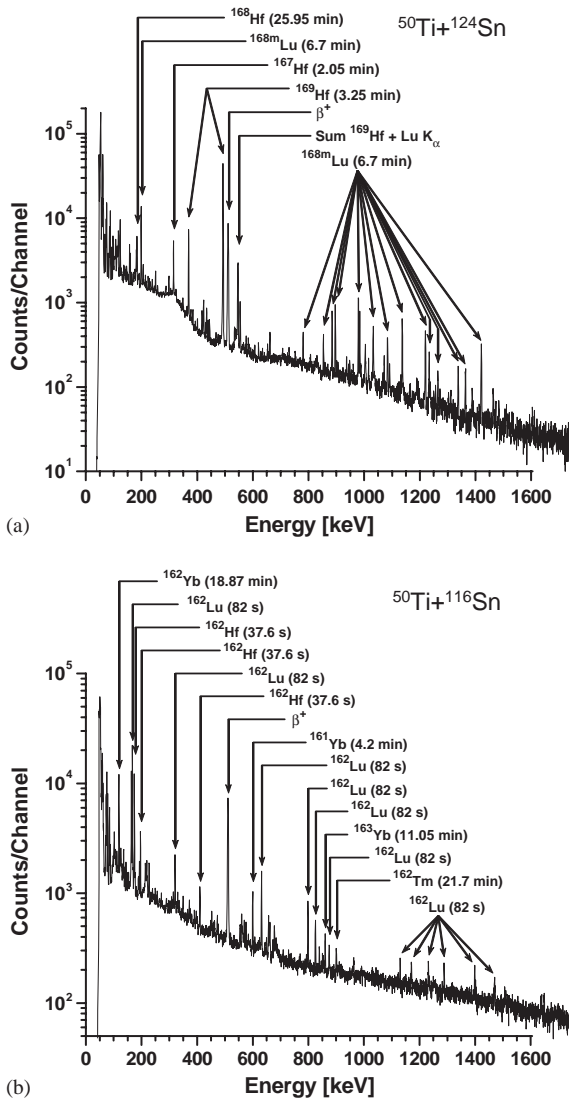


Fig. 4. Same as Fig. 3, but for the nuclear reactions (a)  $^{50}\text{Ti} + ^{124}\text{Sn}$  used for production of  $^{169}\text{Hf}$  ( $T_{1/2} = 3.2$  min) and (b)  $^{50}\text{Ti} + ^{116}\text{Sn}$  used for production of  $^{162}\text{Hf}$  ( $T_{1/2} = 37.6$  s).

and/or (ii) BGS efficiencies is not clear at the moment. Because of the higher rate, the  $^{nat}\text{Ge}$ -based reaction is preferred for chemistry experiments with the group 4 element Zr. It is noteworthy that the reaction  $^{18}\text{O} + ^{74}\text{Se}$  also appears suitable for the production, via pxn reactions, of various short-lived isotopes of the group 5 element niobium (Nb). However, the

almost complete absence of  $\gamma$ -lines from molybdenum (Mo) isotopes, which are formed in xn reactions, indicates that the  $^{18}\text{O} + ^{74}\text{Se}$  reaction is not suited to study this lighter homolog of seaborgium (Sg, element 106).

Fig. 4 clearly shows that the chosen reactions are suitable for producing the desired Hf isotopes. For all investigated reactions, the removal of nuclear transfer products in the BGS is good and only  $\gamma$ -lines attributable to fusion–evaporation products of the expected nuclear reactions and their decay products are identified in the  $\gamma$ -spectra.

## 6. Background reduction through preseparation

As mentioned in the introduction, the only TAN chemistry experiments using preprepared isotopes that have been performed so far [16,17] took advantage of the reduced background. We therefore investigated this aspect by comparing  $\gamma$ -spectra of  $^{169}\text{Hf}$  produced with and without preseparation. In both experiments,  $^{169}\text{Hf}$  was transported to a collection site with a KCl/He aerosol-gas-jet (1.5–1.7 l/min He). The aerosol particles were deposited on a platinum (Pt) disk and then picked up and dissolved in 4 ml of 10 M hydrochloric acid. The solution was placed in front of a HPGe  $\gamma$ -detector and measured for 4 min. In the first experiment,  $^{169}\text{Hf}$  was produced in the reaction  $^{20}\text{Ne} + ^{nat}\text{Sm}$  where the target material was electrodeposited on a Be backing and the recoils were thermalized in a gas volume directly behind the target. This volume was constantly flushed with the KCl-laden He gas. Hence, no physical preseparation was performed. In another experiment with the BGS,  $^{169}\text{Hf}$  was produced in the reaction  $^{50}\text{Ti} + ^{124}\text{Sn}$  using the target described in Section 3.4. The EVRs were separated from the beam and nuclear transfer products in the BGS and guided to the RTC which was flushed with the KCl/He aerosol. Even though many aspects of the two experimental setups, such as the vacuum window, target backing material, target thickness, target assembly, and the nuclear reactions are different, a comparison is justifiable because these experimental situations are close to

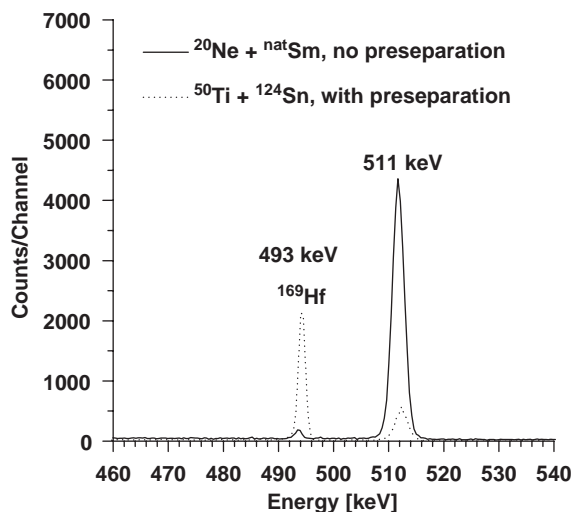


Fig. 5. Comparison of  $\gamma$ -ray spectra showing the 493-keV  $\gamma$ -line of  $^{169}\text{Hf}$  ( $T_{1/2} = 3.2$  min) and the positron annihilation line at 511 keV. The solid line shows the results obtained in an experiment where the nuclear reaction  $^{20}\text{Ne} + ^{\text{nat}}\text{Sm}$  was used to produce  $^{169}\text{Hf}$  without physical preseparation. The dotted line shows the results obtained in another experiment where the nuclear reaction  $^{50}\text{Ti} + ^{124}\text{Sn}$  was used to produce  $^{169}\text{Hf}$  which was physically preseparated in the BGS. The nuclear reaction products were transported with a KCl/He aerosol-gas-jet to a collection site where the aerosol particles were deposited on a Pt disk. The aerosol material was dissolved in 4 ml of 10 M hydrochloric acid. The solution was placed in front of a HPGe  $\gamma$ -detector. The solution was counted for 4 min.

those that are typically used for the production of TANs and their homologs for chemistry experiments. The interesting region of the  $\gamma$ -spectrum around the most intense  $\gamma$ -line of  $^{169}\text{Hf}$  at 493 keV and the positron annihilation peak at 511 keV is displayed in Fig. 5. This improvement in peak-to-background ratio is probably mostly due to the removal in the BGS of  $\beta^+$ -decaying nuclear transfer products and products of reactions of the beam with the target backing and various components of the target assembly.

## 7. Conclusions

The utilization of a heavy-ion beam “cocktail” allows for the chemical investigation of preseparated TANs and their periodic table homologs

under identical conditions. The method overcomes some limitations faced in many chemical investigations of TANs. New classes of chemical systems, such as volatile metal complexes in gas-phase experiments [29] or novel extraction systems like crown ethers [30] become available for study and thus completely new possibilities open up for the field. In this paper, the group 4 elements Zr and Hf, homologs of Rf, are used to illustrate the method. It is applicable to homologous elements within other groups of the periodic table without major alteration. For example, the group 5 elements Nb, tantalum (Ta), and dubnium (Db, element 105) can be produced with a  $^{18}\text{O}^{5+}/^{51}\text{V}^{14+}$  cocktail using the reactions  $^{74}\text{Se}(^{18}\text{O}, \text{p xn})^{87,88}\text{Nb}$ ,  $^{112,116,120,124}\text{Sn}(^{51}\text{V}, \text{xn})^{160-171}\text{Ta}$  and  $^{209}\text{Bi}(^{51}\text{V}, \text{n})^{259}\text{Db}$ .

## Acknowledgments

We thank the staff of the LBNL 88-Inch Cyclotron for providing the stable “cocktail” beams. The EVAPOR calculations for the  $^{18}\text{O}$ -based reactions were carried out by H. Mahmud whom we gratefully acknowledge. A PC version of the HIVAP computer code was provided by R. Dressler. These studies were supported in part by the Swiss National Science Foundation and the Director, Office of Science, Office of High Energy and Nuclear Physics, Division of Nuclear Physics, and the Office of Basic Energy Sciences, Chemical Sciences Division, US Department of Energy under Contract No. DE-AC03-76SF00098.

## References

- [1] M. Schädel (Ed.), The Chemistry of the Superheavy Elements, Kluwer Academic Publishers, Dordrecht, The Netherlands, 2003.
- [2] Y. Nai-Qi, D.T. Jost, U. Baltensperger, H.W. Gäggeler, Radiochim. Acta. 47 (1989) 1.
- [3] H. Wollnik, H.G. Wilhelm, G. Röbig, H. Jungclas, Nucl. Instr. and Meth. A 127 (1975) 539.
- [4] H. Wollnik, Nucl. Instr. and Meth. A 139 (1976) 311.
- [5] A. Türler, B. Eichler, D.T. Jost, D. Piguet, H.W. Gäggeler, K.E. Gregorich, B. Kadkhodayan, S.A. Kreek, D.M. Lee,

- M. Mohar, E. Sylwester, D.C. Hoffman, S. Hübener, *Radiochim. Acta.* 73 (1996) 55.
- [6] G. Skarnemark, J. Alstad, N. Kaffrell, N. Trautmann, *J. Radioanal. Nucl. Chem.* 142 (1990) 145.
- [7] G. Skarnemark, *J. Radioanal. Nucl. Chem.* 243 (2000) 219.
- [8] M. Schädel, W. Brühle, E. Jäger, E. Schimpf, J.V. Kratz, U.W. Scherer, H.P. Zimmermann, *Radiochim. Acta.* 48 (1989) 171.
- [9] I. Zvara, A.B. Yakushev, S.N. Timokhin, X. Honggui, V.P. Perelygin, Yu.T. Chuburkov, *Radiochim. Acta.* 81 (1998) 179.
- [10] Ch.E. Düllmann, W. Brühle, R. Dressler, K. Eberhardt, B. Eichler, R. Eichler, H.W. Gäggeler, T.N. Ginter, F. Glaus, K.E. Gregorich, D.C. Hoffman, E. Jäger, D.T. Jost, U.W. Kirbach, D.M. Lee, H. Nitsche, J.B. Patin, V. Pershina, D. Piguet, Z. Qin, M. Schädel, B. Schausten, E. Schimpf, H.-J. Schött, S. Soverna, R. Sudowe, P. Thörle, S.N. Timokhin, N. Trautmann, A. Türlér, A. Vahle, G. Wirth, A.B. Yakushev, P.M. Zielinski, *Nature* 418 (2002) 859.
- [11] Ch.E. Düllmann, B. Eichler, R. Eichler, H.W. Gäggeler, D.T. Jost, D. Piguet, A. Türlér, *Nucl. Instr. and Meth. A* 479 (2002) 631.
- [12] A. v. Zweidorf, R. Angert, W. Brühle, S. Bürger, K. Eberhardt, R. Eichler, H. Hummrich, E. Jäger, H.-O. Kling, J.V. Kratz, B. Kuczewski, G. Langrock, M. Mendel, U. Rieth, M. Schädel, B. Schausten, E. Schimpf, P. Thörle, N. Trautmann, K. Tsukada, N. Wiehl, G. Wirth, *Radiochim. Acta.* 92 (2004) 855.
- [13] E.V. Fedoseev, M.I. Aizenberg, S.N. Timokhin, S.S. Travnikov, I. Zvara, A.V. Davydov, B.F. Myasedov, *J. Radioanal. Nucl. Chem. Lett.* 119 (1987) 347.
- [14] I. Zvara, Yu.T. Chuburkov, V.Z. Belov, G.V. Buklanov, B.B. Zakhvataev, T.S. Zvarova, O.D. Maslov, R. Caletka, M.R. Shalaevsky, *J. Inorg. Nucl. Chem.* 32 (1970) 1885.
- [15] U.W. Kirbach, C.M. Folden III, T.N. Ginter, K.E. Gregorich, D.M. Lee, V. Ninov, J.P. Omtvedt, J.B. Patin, N.K. Seward, D.A. Strellis, R. Sudowe, A. Türlér, P.A. Wilk, P.M. Zielinski, D.C. Hoffman, H. Nitsche, *Nucl. Instr. and Meth. A* 484 (2002) 587.
- [16] J.P. Omtvedt, J. Alstad, H. Breivik, J.E. Dyve, K. Eberhardt, C.M. Folden III, T. Ginter, K.E. Gregorich, E.A. Hult, M. Johansson, U.W. Kirbach, D.M. Lee, M. Mendel, A. Nähler, V. Ninov, L.A. Omtvedt, J.B. Patin, G. Skarnemark, L. Stavsetra, R. Sudowe, N. Wiehl, B. Wierczinski, P.A. Wilk, P.M. Zielinski, J.V. Kratz, N. Trautmann, H. Nitsche, D.C. Hoffman, *J. Nucl. Radiochem. Sci.* 3 (2002) 121.
- [17] L. Stavsetra, K.E. Gregorich, J. Alstad, H. Breivik, K. Eberhardt, C.M. Folden III, T.N. Ginter, M. Johansson, U.W. Kirbach, D.M. Lee, M. Mendel, L.A. Omtvedt, J.B. Patin, G. Skarnemark, R. Sudowe, P.A. Wilk, P.M. Zielinski, H. Nitsche, D.C. Hoffman, J.P. Omtvedt, *Nucl. Instr. and Meth. A* 543 (2005) 509.
- [18] V. Ninov, K.E. Gregorich, C.A. McGrath, in: B.M. Sherrill, D.J. Morrissey, C.N. Davids (Eds.), *Proceedings of the Conference on Exotic Nuclei and Atomic Masses, ENAM98; AIP Conf. Proc.* 455 (1998) 704.
- [19] J.P. Omtvedt, J. Alstad, K. Eberhardt, K. Fure, R. Malmbeck, M. Mendel, A. Nähler, G. Skarnemark, N. Trautmann, N. Wiehl, B. Wierczinski, *J. Alloys Comp.* 271–273 (1998) 303.
- [20] D. Leitner, M.A. McMahan, D. Argento, T. Gimpel, A. Guy, J. Morel, C. Siero, R. Thatcher, C.M. Lyneis, E.O. Lawrence Berkeley National Laboratory, LBNL-Report 51451 (2002), Berkeley, CA; and in: *Proceedings of the 15th International Workshop on ECR Ion Sources, ECRIS '02, Jyväskylä, Finland, June 12–14, 2002*, p. 183.
- [21] C. Lyneis, *Nucl. Instr. and Meth. B* 10/11 (1985) 775.
- [22] W. Reisdorf, M. Schädel, *Z. Phys. A* 343 (1992) 47.
- [23] R. Dressler, Paul Scherrer Institut, PSI Scientific Report 1988/vol 1, Villigen, Switzerland, 1999, p. 131, ISSN:1423–7296.
- [24] J.R. Beene, N.G. Nicolis, computer code EVAPOR (unpublished); evolved from the code PACE by A. Gavron, *Phys. Rev. C* 21 (1980) 230.
- [25] K.E. Gregorich, T.N. Ginter, W. Loveland, D. Peterson, J.B. Patin, C.M. Folden III, D.C. Hoffman, D.M. Lee, H. Nitsche, J.P. Omtvedt, L.A. Omtvedt, S. Stavsetra, R. Sudowe, P.A. Wilk, P.M. Zielinski, K. Aleklett, *Eur. Phys. J. A* 18 (2003) 633.
- [26] F.P. Hessberger, S. Hofmann, V. Ninov, P. Armbruster, H. Folger, G. Münzenberg, H.J. Schött, A.G. Popeko, A.V. Yeremin, A.N. Andreyev, S. Saro, *Z. Phys. A* 359 (1997) 415.
- [27] J.F. Ziegler, *Nucl. Instr. and Meth. A* 219–220 (2004) 1027.
- [28] J.B. Moulton, J.E. Stephenson, R.P. Schmitt, G.J. Wozniak, *Nucl. Instr. and Meth.* 157 (1978) 325.
- [29] Ch.E. Düllmann, G.K. Pang, C.M. Folden III, K.E. Gregorich, D.C. Hoffman, H. Nitsche, R. Sudowe, P.M. Zielinski, in: S.M. Qaim, H.H. Coenen (Eds.), *Advances in Nuclear and Radiochemistry, General and Interdisciplinary, Vol. 3*, Jülich, Germany, 2004, pp. 147–149.
- [30] R. Sudowe, Ch.E. Düllmann, L.M. Farina, C.M. Folden III, K.E. Gregorich, S.E.H. Gallaher, D.C. Hoffman, D.C. Phillips, J.M. Schwantes, R.E. Wilson, P.M. Zielinski, H. Nitsche, in: S.M. Qaim, H.H. Coenen (Eds.), *Advances in Nuclear and Radiochemistry, General and Interdisciplinary, Vol. 3*, Jülich, Germany, 2004, pp. 144–146.